

Value of formalin fixation for the prolonged preservation of rodent myocardial microanatomical organization: Evidence by MR diffusion tensor imaging

Archontis Giannakidis^{1,2,3}, Grant T Gullberg^{3,4}, Dudley J Pennell^{1,2},
David N Firmin^{1,2}

1. NIHR Cardiovascular Biomedical Research Unit, Royal Brompton Hospital, London, UK
2. National Heart & Lung Institute, Imperial College London, London, UK
3. Life Sciences Division, Lawrence Berkeley National Laboratory, Berkeley, California, USA
4. Department of Radiology & Biomedical Imaging, University California San Francisco, San Francisco, California, USA

Corresponding author: Archontis Giannakidis

Email: A.Giannakidis@rbht.nhs.uk

Tel: +44(0)2073518819

Fax: +44(0)2073518816

Address: Cardiovascular Biomedical Research Unit, Royal Brompton Hospital, Sydney Street, London, SW3 6NP, UK

Running title: Preserving cardiac microanatomy in formalin

Grant information: (i) Grant Sponsor: National Institutes of Health, Grant Number: R01 EB007219. (ii) Grant Sponsor: Director, Office of Science, Office of Biological and Environmental Research, Biological Systems Science Division of the U.S. Department of Energy, Grant Number: DE-AC02-05CH11231. (iii) Grant Sponsor: NIHR Cardiovascular Biomedical Research Unit of Royal Brompton & Harefield NHS Foundation Trust and Imperial College London, Grant Number: -.

This article has been accepted for publication and undergone full peer review but has not been through the copyediting, typesetting, pagination and proofreading process which may lead to differences between this version and the Version of Record. Please cite this article as an 'Accepted Article', doi: 10.1002/ar.23359

ABSTRACT

Previous *ex vivo* diffusion tensor imaging (DTI) studies on formalin fixed myocardial tissue assumed that, after some initial changes in the first 48 hours since the start of fixation, DTI parameters remain stable over time. Prolonged preservation of cardiac tissue in formalin prior to imaging has been seen many times in the DTI literature as it is considered orderly. Our objective is to define the effects of the prolonged cardiac tissue exposure to formalin on tissue microanatomical organization, as this is assessed by DTI parameters. DTI experiments were conducted on eight excised rodent hearts that were fixed by immersion in formalin. The samples were randomly divided into two equinumerous groups corresponding to shorter (~2 weeks) and more prolonged (~ 6-8 weeks) durations of tissue exposure to formalin prior to imaging. We found that when the duration of cardiac tissue exposure to formalin before imaging increased, water diffusion became less restricted, helix angle (HA) histograms flattened out and exhibited heavier tails (even though the classic HA transmural variation was preserved), and a significant loss of inter-voxel primary diffusion orientation integrity was introduced. The prolonged preservation of cardiac tissue in formalin profoundly affected its microstructural organization, as this was assessed by DTI parameters. The accurate interpretation of diffusivity profiles necessitates awareness of the pitfalls of prolonged cardiac tissue exposure duration to formalin. The acquired knowledge works to the advantage of a proper experimental design of DTI studies of fixed hearts.

Key words: Magnetic resonance diffusion tensor imaging; rat myocardial microanatomy; formalin; fixation; diffusivity; diffusion anisotropy; helix angle; inter-voxel diffusion coherence.

INTRODUCTION

Magnetic resonance diffusion tensor imaging (MR-DTI), also known as DTI, has emerged (Basser et al., 1994) as a powerful non-invasive tool for mapping the orientation-dependent microanatomical organization of the myocardium. To do so, it elegantly relates the self-diffusion of water molecules that undergo Brownian motion to proton spin relaxation MR signals.

DTI calls for prolonged scanning times owing to the fact that (i) a minimum of seven acquisitions are required, (ii) averaging of multiple acquisitions is typically applied to improve the inherently low signal-to-noise ratio (SNR) thanks to the diffusion encoding being a negative contrast mechanism (Hsu et al., 2009). In addition, measuring diffusion in a beating heart is liable to motion-induced artifactual signal loss during the diffusion encoding. For these reasons, most cardiac DTI studies have been conducted in *ex vivo* conditions using excised hearts, especially when three-dimensional (3D) high spatial resolution whole organ data were required (Lombaert et al., 2012).

To prevent excised hearts (and other biological tissues) from degradation, chemical fixation (CF) of the sample has been a common laboratory practice. To ensure that the *postmortem* tissue represents the structural characteristics of the *in vivo* tissue as accurately as possible, it is of critical importance to minimize delays in the start of the fixation process after death (Dyrby et al., 2011; Eggen et al., 2012).

Among the various available fixatives, 10% neutral buffered formalin, often shortened to formalin, has been by far the most widely used solution for many decades (Werner et al., 2000). Formalin is a non-coagulative additive liquid mixture comprising phosphate salts, distilled water

and approximately 4% formaldehyde. It stabilizes both structure and metabolism of biological tissues by cross-linking proteins (Werner et al., 2000). Its huge popularity relies on its low cost, ease of preparation, rapid tissue penetration, excellent prolonged preservation of tissue morphological details, and capacity to circumvent pigment formation as a result of its neutral pH (Carleton, 1980; Werner et al., 2000; Dyrby et al., 2011).

In the related literature that deals with 3D high spatial resolution DTI studies of excised fixed hearts, one may witness a great variation in the duration of tissue exposure to formalin before imaging, spanning from 48 hours to over a year. While a minimum exposure duration (of ~24-48 hours, depending on the specimen size) needs to be ensured (Carleton, 1980; Fox et al., 1985; Srinivasan et al., 2002; Webster et al., 2009) to allow for formalin to penetrate tissue and chemical reactions (i.e., formaldehyde group binding to proteins) to complete, previous *ex vivo* cardiac DTI studies have assumed that the prolonged tissue exposure to formalin does not alter the parameters used to characterize microstructural organization. The bases for this assumption were: (i) Histology-based experimental observations (Fox et al., 1985) that the tissue reaches an equilibrium state after the initial crosslinking actions, and (ii) former findings from some individual non-cardiac longitudinal studies (Kim et al., 2009; Dyrby et al., 2011) demonstrating stability of DTI parameters over a prolonged (namely, several weeks for cervical spinal cord and three years for brain) period of tissue exposure to formalin. A recent cardiac DTI study (Watson and Hsu, 2012) that aimed at evaluating the effects of fixation duration on DTI parameters showed that, after some initial changes (that took place the first 48 hours following the tissue immersion in the formaldehyde-based solution), the DTI parameters remained stable for up to seven days; however, it happens frequently (Jiang et al., 2007; Eggen et al., 2012; Mazumder et

al, 2013a,b; Abdullah et al., 2014) that the cardiac tissue is exposed to formalin for a much more prolonged period prior to imaging.

In summary, in spite of numerous *ex vivo* DTI studies using heart samples that were stored in formalin for either shorter or more prolonged time intervals before imaging, little is known regarding the effects of the fixation duration on DTI-derived parameters used to characterize cardiac tissue microstructure. The need for research into how the time interval of cardiac tissue exposure to formalin prior to imaging affects its diffusion magnetic resonance imaging (MRI) properties has been also recognised by other recent studies (Hales et al., 2011; Eggen et al., 2012).

In the present study, we use excised rodent hearts that were fixed by immersion in formalin to assess the effects of fixation duration on DTI-derived parameters that portray tissue microstructure. Such knowledge is of multifaceted importance, in that: (i) It works to the advantage of a proper experimental design of DTI studies of fixed myocardial specimens by providing unambiguous guidelines for specimen preparation. This is crucial for a prospective researcher who needs to be aware of all the potential contributing factors ahead of designing a project. (ii) It favours the accurate interpretation of the results, as well as their rigorous comparison across multiple populations, through avoiding pitfalls of misguided readings. (iii) The duration of exposure to fixative is one of the first steps of tissue handling, so it arguably dictates the quality of the final DTI results more than other steps that follow do. In addition to the above three factors, the increasing availability (Guilfoyle et al., 2003) of biological tissue specimen banks renders this knowledge even more valuable nowadays.

MATERIALS AND METHODS

Research Animal Model

We performed *ex vivo* studies on eight ($N=8$) Wistar Kyoto (WKY) aged male rats, obtained from an unrelated study (Hernandez et al., 2013). The WKY rat is a well-established animal model of normal non-pathologic cardiac behaviour. The rats were bought from Charles River Laboratories (Charles River Laboratories International, Inc., Wilmington, MA, USA). All animal procedures conformed to the guidelines set forth by the Animal Welfare and Research Committee of Lawrence Berkeley National Laboratory.

Heart Preparation

The rats were anaesthetized via deep isoflurane inhalation. The intact hearts were rapidly dissected and flushed with warmed isotonic saline. As soon as each excised heart had been rinsed clean of blood, it was weighed and instantaneously immersed in 60cc of the fixative solution, where it was stored at room temperature until imaging. For this study, 10% neutral buffered formalin (Sigma-Aldrich Corp., St. Louis, MO, USA) with pH=6.9-7.1 and osmolality=1240-1360 milliosmoles/kg (Henwood, 2010) was used. All hearts were arrested in end diastole.

Other Study Design

To assess the impact of the length of cardiac tissue exposure time to formalin prior to imaging on DTI-derived parameters used to characterize microstructural organization, the excised samples were randomly divided into two equinumerous groups corresponding to different durations of tissue exposure to formalin prior to imaging: (i) The first study group comprised excised rat hearts ($N=4$) that were stored in formalin for a shorter time interval (but

long enough to allow for the fixation process to complete (Wu et al., 2007; Wu et al., 2009; Watson and Hsu, 2012; Abdullah et al., 2014), approximately 2 weeks (range: 14-15 days). (ii) The second group comprised excised rat hearts ($N=4$) that remained in formalin for a more prolonged time interval, approximately 6-8 weeks (range: 41-58 days).

Imaging

Whole heart imaging was conducted on a Bruker BioSpec 7T horizontal bore MRI scanner (Bruker Biospin, Ettlingen, Germany) interfaced with the Paravision 5.1 software package. All MRI acquisitions were performed at typical room temperature, approximately 20°C.

For imaging, each heart was placed in a sealed 5 ml standard syringe filled with Fomblin (Solvay Solexis, Inc., West Deptford, NJ, USA) to increase contrast and eliminate susceptibility artifacts near the boundaries of the myocardium. Hearts were secured inside the containers using gauze to prevent the specimen from floating in the container. The long axis of each heart was aligned with the x -axis of the scanner. A custom-made radio frequency (RF) coil (single turn solenoid, wrapped around the syringe) was used for signal transmission and reception.

To acquire DTI data, a standard 3D spin echo readout sequence was used with the following parameters: echo time (TE) = 19.224ms, pulse repetition time (TR) = 500ms. The field of view (FOV) was 27×15.5×15.5 (mm), with a data matrix size = 169×97×97, resulting in an isotropic resolution of 0.160mm.

Diffusion encoding was carried out using a pair of trapezoidal gradient pulses with parameters: gradient duration (δ) = 4ms, inter-gradient separation (Δ) = 10ms, rise time = 0.25ms, maximum strength of the gradient pulse (G) = 30G/cm, resulting in a nominal b value of 1000s/mm², accounting for all imaging gradients and cross-terms between imaging and diffusion

gradients. The diffusion-induced signal decay was measured along 12 optimized (Papadakis et al., 1999) directions. All diffusion measurements were preceded by the acquisition of one reference (B0) image. The number of signal averages that was acquired was one and the total scan duration for each heart was approximately 17 hours.

Analyses

At first, the effective diffusion tensor D at each voxel was estimated by applying a nonlinear least-squares fitting algorithm (Koay et al., 2006) to the diffusion-weighted measurements S_i ($i = 1, \dots, N_g$). After acquiring the six independent elements of D , the three eigenvalues d_1, d_2, d_3 (where $d_1 \geq d_2 \geq d_3$), and the corresponding eigenvectors e_1, e_2, e_3 were calculated at each voxel by performing tensor diagonalization. The eigenvectors represent the three principal axes of diffusion, whereas each eigenvalue is equal to the rate of diffusion along the direction that the paired eigenvector points.

The longitudinal diffusivity (λ_L), transverse diffusivity (λ_T), mean diffusivity (MD), and fractional anisotropy (FA) were subsequently derived from the three eigenvalues using the following formulae, respectively:

$$\lambda_L = d_1 \quad (1)$$

$$\lambda_T = \frac{d_2 + d_3}{2} \quad (2)$$

$$\text{MD} = \frac{d_1 + d_2 + d_3}{3} \quad (3)$$

$$\text{FA} = \sqrt{\frac{3[(d_1 - \text{MD})^2 + (d_2 - \text{MD})^2 + (d_3 - \text{MD})^2]}{2[d_1^2 + d_2^2 + d_3^2]}} \quad (4)$$

Since it was shown (Hsu et al., 1998) that the primary eigenvector of the diffusion tensor coincides with the local myocyte orientation, then, λL represents the water diffusivity parallel to the long axes of myocytes, while λT corresponds to water diffusivity perpendicular to the axonal myocardial cells.

Apart from the magnitude and degree of anisotropy of water diffusion, its orientation was also studied. To this end, helix angle (HA) maps were estimated, where helix angle is defined (Streeter et al., 1969) as the angle between the cardiac short-axis plane and the projection of the primary eigenvector onto the epicardial tangent plane. Such maps have been frequently employed to characterize the classic (Hsu et al., 2009) helix-like orientation pattern of the myocytes within the left ventricular wall.

Finally, we sought to assess the inter-voxel primary diffusion orientation coherence. To quantitatively map the level of principal diffusion orientation integrity, within a given voxel neighbourhood, we relied on the inter-voxel diffusion coherence index (IVDC) (Wang et al., 2008). This DTI-derived vector homogeneity measure has been also employed in the past (Giannakidis et al., 2012) to gauge the extent of orientation derangement of the normal myocardial patterns associated with hypertensive hypertrophy. In contrast to other measures of primary eigenvector dispersion applied in the DTI literature such as the coherence index (Klingberg et al., 1999), IVDC has the supplementary favourable quality that it is insensitive to the inherent eigenvector sign ambiguity (Beg et al., 2007). Below, we briefly describe the process of acquiring IVDC with respect to the primary eigenvector for our cardiac DTI study.

IVDC is a scatter matrix-based tool, so let us first define the scatter matrix. Consider an arbitrary voxel (i, j, k) that belongs to the cardiac wall, and a local area that consists of the voxel itself and its 26 nearest neighbours that span in the same short-axis cardiac slice and the slices

right above and below. Then, the scatter matrix $M(i,j,k)$ for the specific area is a symmetric positive semidefinite second-order dyadic tensor of size 3x3 given by

$$M(i,j,k) \equiv \frac{1}{27} \sum_{l=i-1}^{i+1} \sum_{m=j-1}^{j+1} \sum_{n=k-1}^{k+1} (\mathbf{e}_{1l,m,n} \cdot \mathbf{e}_{1l,m,n}^T) \quad (6)$$

where $\mathbf{e}_{1l,m,n}$ is the major eigenvector at the (l,m,n) voxel. Finally, the IVDC index is given by

$$\text{IVDC}(i,j,k) \equiv \frac{\sqrt{(t_1 - t)^2 + (t_2 - t)^2 + (t_3 - t)^2}}{t\sqrt{6}} \quad (7)$$

where t_1, t_2, t_3 are the eigenvalues of $M(i,j,k)$ and t is the mean of these eigenvalues. IVDC is normalized such that it takes values between 0 and 1. A large value of this index at a specific voxel indicates a uniform primary water diffusion orientation distribution in this voxel's neighborhood. On the other hand, smaller values of IVDC reflect a regional loss of the primary water diffusion orientation organization.

Region of Interest - Segmentation

The short-axis cardiac slice with the largest area (in the mid left ventricular region) was analyzed for each heart of the two study groups. The left ventricular wall was segmented semi-automatically using cubic splines (de Boor, 1978). The region of interest (ROI) was isolated in the B0 image. Extra care was taken to exclude papillary muscles and areas of signal dropout. Any voxel, at which the diffusion tensor diagonalization resulted in at least one negative eigenvalue, was excluded on thermodynamic grounds. The SNR was measured in the B0 images, as the quotient of the mean signal intensity of the myocardium divided by the standard deviation of the largest possible ROI placed in the image background.

Statistical Analysis

The mean and standard deviation measures of λL , λT , MD, FA, and IVDC parameter values over all the voxels within the ROI were computed and reported for every rat heart of the two study groups. To test the statistical significance of the differences in the parameter mean values between the two groups, the nonparametric Mann-Whitney test was employed. A value of $p < 0.05$ was considered to be statistically significant. Mean SNR values and HA probability density functions (PDFs), averaged over the four hearts of each group, were also computed and compared.

All post-processing computations described in Materials and Methods section were performed using custom-made code written in Matlab (Mathworks, Natick, MA, USA).

RESULTS

There was no statistically significant difference in the age of the rats at the time of heart excision ($p = 0.8857$) and the heart weight to body weight ratio ($p = 0.9714$) between the two groups.

It was observed (Fig.1a) that extended exposure to formalin introduced a statistically significant ($p < 0.05$) increase in measured λT , when compared to shorter exposure duration. λL demonstrated (Fig.1b) a similar trend, but the changes did not reach the statistical significance level ($p = 0.1143$). As a result of the λT and λL changes, a statistically significant ($p < 0.05$) increase in measured MD (Fig.1c) and a statistically significant ($p < 0.05$) decrease in measured FA (Fig.1d) were noted after increasing the tissue exposure to formalin prior to imaging. As an

interim summary, we found that water diffusion in the myocardium became less restricted as tissue storage time to formalin before imaging increased.

The classic transition of HAs (namely, from negative values at the epicardium to zero at the mesocardium to positive values at the endocardium) was preserved (Fig.2) after increasing the cardiac tissue exposure time to formalin before imaging. However, by inspecting (Fig.3) the resulting HA probability density functions (PDFs), it may be seen that the prolonged exposure to fixative resulted in a flatter density with heavier tails. Additionally, it was observed (Fig.4) that the prolonged tissue exposure to formalin prior to imaging caused a statistically significant ($p < 0.05$) loss of the primary water diffusion orientation integrity. Finally, data-sets from the samples that remained to formalin for more prolonged period presented higher SNR values (range=130-155, mean=143) compared with data-sets from samples that were exposed to formalin for shorter period (range=107-137, mean=119), but the changes did not reach the statistical significance level ($p=0.0571$).

A summary of the quantitative results of this study is presented in Table 1.

DISCUSSION AND CONCLUSIONS

The Main Contribution of this Study

Cardiac DTI's sensitivity to the duration of tissue exposure to formalin prior to imaging is still not well characterized. The objective of this study was to determine whether cardiac samples that were exposed to formalin for a more prolonged period (~ 6-8 weeks) before imaging preserved microstructural organization, compared to samples stored in formalin for a shorter period (~2 weeks) prior to imaging.

The key findings of this study were: (i) Water diffusion in the myocardium became much less restricted as the duration of tissue exposure to formalin prior to imaging increased, as indicated by the statistically significant increases in λT and MD, and the statistically significant decrease in FA. λL also increased, but the changes did not reach the statistical significance level. (ii) The classic transition of HAs (namely, from negative values at the epicardium to zero at the mesocardium to positive values at the endocardium) was preserved after increasing the cardiac tissue exposure time to formalin before imaging. However, the resulting HA histogram flattened out and exhibited heavier tails. The heavier distribution tails mirror the notable increase in the longitudinally-oriented myocytes. (iii) The prolonged tissue exposure to formalin prior to imaging introduced a significant loss of inter-voxel primary water diffusion orientation integrity. Such abrupt changes and discontinuities between neighboring voxels do not resonate with the knowledge (acquired through invasive histology studies (Streeter et al., 1969)) of the smooth transmural variation in myocyte orientations within a healthy left ventricular wall. In addition, the fact that the SNR values were not different between the two groups, corroborates the assertion that the measured changes in the primary eigenvector orientation integrity represent actual structural changes, rather than an artefact of the measurement process.

Our results from the shorter fixation period samples appear comparable to the limited number of related studies that employed fixation periods shorter than two weeks. Similar FA values (0.25-0.28) were reported by Hales et al. (Hales et al., 2011), imaging Sprague Dawley rat hearts 24 hours post-fixation. Gilbert et al. (Gilbert et al., 2013) showed similar HA transmural variation in a Wistar rat heart imaged 2 hours post-fixation. Other DTI studies with fixation periods shorter than two weeks (Mazumder et al., 2013c; Watson and Hsu, 2012) have used different species and imaging protocols making comparisons difficult.

This study has many important implications: (i) The duration of cardiac tissue exposure to formalin before imaging profoundly affected the measured water diffusion magnitude, degree of anisotropy, and orientation. Such an important limiting parameter value should not be missing from the description of the experimental set-up, as is the case in many related studies (Chen et al., 2003; Walker et al., 2005; Helm et al., 2006; Li et al., 2009). (ii) Contrary to the related community's current conception, changes in the DTI-derived cardiac microstructure keep on taking place beyond the initial 48 hours following the tissue immersion in formalin. (iii) The results question the use of DTI in microstructural studies of cardiac samples exposed to formalin for a prolonged period that exceeds six weeks prior to imaging. In fact, there are numerous *ex vivo* cardiac DTI studies, where the specimens remained in formalin for a prolonged period (for example, over a month in (Jiang et al., 2007; Abdullah et al., 2014), six months in (Mazumder et al., 2013a,b), over a year in (Eggen et al., 2012), to name a few) prior to imaging. According to the findings of this paper, caution should be exercised in adopting the results from such studies. The accurate interpretation of diffusivity profiles necessitates awareness of the pitfalls of prolonged tissue exposure duration to formalin before imaging. The widespread use of cardiac (and other) chemically-fixed tissue samples for time-intensive high-resolution diffusion MRI studies entails the standardization of the optimal amount of tissue exposure time to formalin (as well as other fixation details).

Biochemical Interpretation of the Results

Despite the fact that the biochemical mechanisms underlying fixation have not been sufficiently elucidated (Fox et al., 1985; Schmierer et al., 2008), next, we try to explain the findings of this study.

It was noted that the prolonged cardiac tissue exposure to formalin ahead of imaging induced greater increases in the transversal than longitudinal measured diffusivities, when compared with the shorter fixation period. Such advances possibly reflect (Eggen et al., 2012) the myocyte membrane degradation, and thus increased membrane permeability, following the prolonged fixation time. Indeed, it has been demonstrated (Shepherd et al., 2009) that by increasing the period of tissue exposure to a formaldehyde-based aqueous solution, this results in depletion of lipid membranes through reactions with carbon double bonds. Finally, the observed changes in the measured primary water diffusion orientation may relate to the extreme osmotic pressures exerted by formalin onto the myocytes (Fox et al., 1985; Hales et al., 2011).

Temperature Control

No discussion of water molecular motion would be complete without mentioning temperature, as changes in environmental temperature may bias (Kim et al., 2009; Dyrby et al., 2011) diffusivity measurements. In this study, constant temperature ($\sim 20^{\circ}\text{C}$) was maintained throughout the tissue handling and imaging experiments. Therefore, it is unlikely that temperature differences underlie the measured diffusivity differences between the two study groups.

All hearts of this study were fixed and preserved at room temperature, as colder temperatures encourage (Cromey and Lantz, 2015) the formation of trioxymethylene with a resulting white precipitate, while hotter temperatures generate (Carleton, 1980) formaldehyde fumes.

Tissue Decomposition

To halt the tissue decomposition process, specimens should be immersed in a fixative as rapidly as possible once they are dead. Particularly for cardiac microstructural organization, it has been shown (Eggen et al., 2012) that delays greater than three days in the start of the fixation process compromise DTI measurements. In this study, the time lapse between animal sacrifice and tissue immersion in formalin was insignificant. Consequently, it is unlikely that the measured differences are the result of the tissue decomposition process.

Different Types of Fixative & Chemical Fixation

The current study design used 10% formalin and the immersion fixation method to assess the effects of the ahead of imaging duration of cardiac tissue exposure to the fixative solution on the DTI-derived microstructural organization. However, it should be noted that other types of fixatives (for example coagulants, or combinations (Hales et al., 2011) of formaldehyde and glutaraldehyde) and fixation techniques (for example, perfusion fixation) also exist, and the different types of fixative and fixation method are likely to affect the diffusion MRI properties of the tissue differently (Shepherd et al., 2009; Webster et al., 2009). The impact of the fixative and chemical fixation type should be independently evaluated. The analysis tools used in this paper could prove valuable for such a study that would aim at evaluating the performance of the various fixatives and fixation methods.

Juxtaposition of Fixed & Freshly Excised/*In Vivo* Cardiac Tissue: Not the Theme of this Paper

In the wake of reported (Fox et al., 1985) changes occurring in the tissue physical characteristics during the CF process, there remains a concern that the DTI results of fixed hearts

might not remain relevant for interpreting the *in vivo* tissue microstructural organization. Indeed, a few studies attempted to address the question whether one can extrapolate cardiac DTI results from fixed to freshly excised tissue, but the results were conflicting. That is to say, on the one hand, Mazumder et al. (2013c) demonstrated that formalin fixation resulted in the cardiomyocyte diffusion pattern becoming more isotropic, while, on the other hand, Gilbert et al. (2013) found no changes in cardiac microstructure following the formalin fixation process. In spite of the cardiac DTI parameter comparison between the *ex vivo* and *in vivo* settings being beyond the scope of this paper, the results obtained in this study (from the samples that remained in formalin for a shorter time period) appear to resonate with *in vivo* cardiac DTI results (Chen et al., 2004) acquired from the same animal. Further research is required to establish whether DTI parameters measured in fixed cardiac tissue preserve the same information as in freshly excised/*in vivo* tissue.

Comparison with Non-cardiac Tissues

In marked contrast to the results presented in this paper, two non-cardiac longitudinal studies (Kim et al., 2009; Dyrby et al., 2011) demonstrated stability of DTI parameters over a prolonged (namely, several weeks for cervical spinal cord and three years for brain) period of tissue exposure to formalin. The exact reasons for this discrepancy are unclear. One possibility is that deviations in the tissue preparation by the different organizations may have affected significantly the molecular profile of the tissues. An additional likely cause for this inconsistency may be the different composition of different tissues/species.

Limitations of this Study

A main weakness of this study was the relatively small sample size. Additionally, the effects of fixation duration were juxtaposed on DTI parameters from different animals, rather than multiple DTI measurements from the same animal. Subsequently, a further limitation of this study was that we were not able to acquire DTI data-sets for fixation durations between two and six weeks, and therefore we could not determine with precision any fixation duration where the microstructure changes take place or whether the change is more gradual over this period. Despite these limitations, the distinctness of the measured fixation duration effects was highlighted by the observed statistically significant differences between the two study groups.

A further cardiac study that measures the DTI changes at multiple time points following fixation in the same specimens should be performed to determine the period of stability for formalin fixation. Therefore, until such a study is performed, we recommend researchers (i) use caution when performing DTI evaluations of cardiac tissue that has been exposed to formalin for more than two weeks prior to imaging, and (ii) avoid using heart samples exposed to formalin for six weeks or longer.

In Conclusion

Ex vivo DTI of rodent hearts, that were fixed by immersion in formalin, demonstrated significant differences in the measured water diffusion magnitude, degree of anisotropy, and orientation between samples that had been preserved in formalin for shorter (namely, ~2 weeks) and more prolonged (namely, ~6-8 weeks) time period prior to imaging. Contrary to the related community's current conception, it was found that changes in the DTI-derived cardiac microstructure keep on taking place beyond the initial 48 hours following the tissue immersion in formalin. The results suggest that the prolonged preservation of cardiac tissue in formalin has

detrimental effects on its microstructural organization, as this is assessed by DTI. This study questions the use of DTI in microstructural evaluations of cardiac samples exposed to formalin for a prolonged period prior to imaging. The accurate interpretation of diffusivity profiles necessitates awareness of the pitfalls of the prolonged tissue exposure duration to formalin before imaging.

ACKNOWLEDGEMENTS

The authors would like to thank Kathleen M. Brennan of Lawrence Berkeley National Laboratory for preparation of the excised heart samples. We also thank Osama M. Abdullah and Edward W. Hsu of University of Utah for acquiring the DTI data-sets used in this paper. Many thanks go to Andrew D. Scott, Pedro F. A. D. C. Ferreira, Iain Pierce and Karen McCarthy of Royal Brompton Hospital for fruitful discussions.

This work was supported by funds from: (i) the National Institutes of Health under Grant R01 EB007219, (ii) the Director, Office of Science, Office of Biological and Environmental Research, Biological Systems Science Division of the U.S. Department of Energy under Contract No. DE-AC02-05CH11231, (iii) the NIHR Cardiovascular Biomedical Research Unit of Royal Brompton & Harefield NHS Foundation Trust and Imperial College London.

LITERATURE CITED

- Abdullah OM, Drakos SG, Diakos NA, Wever-Pinzon O, Kfoury AG, Stehlik J, Selzman CH, Reid BB, Brunisholz K, Verma DR, Myrick C, Sachse FB, Li DY, Hsu EW. 2014. Characterization of diffuse fibrosis in the failing human heart via diffusion tensor imaging and quantitative histological validation. *NMR Biomed* 27(11):1378–1386.
- Basser PJ, Mattiello J, LeBihan D. 1994. MR diffusion tensor spectroscopy and imaging. *Biophys J* 66(1):259–267.
- Beg MF, Dickie R, Golds G, Younes L. 2007. Consistent realignment of 3D diffusion tensor MRI eigenvectors. In: *Proceedings of SPIE Medical Imaging*. Vol. 651242. p 1–9.
- de Boor C. 1978. A practical guide to splines. *Applied Mathematical Sciences*. Vol. 27. New York, Berlin: Springer-Verlag.
- Carleton HM. 1980. *Carleton's histological technique*. 5th ed. Oxford, New York: Oxford University Press.
- Chen J, Song SK, Liu W, McLean M, Allen JS, Tan J, Wickline SA, Yu X. 2003. Remodeling of cardiac fiber structure after infarction in rats quantified with diffusion tensor MRI. *Am J Physiol Heart Circ Physiol* 285(3):H946–954.
- Chen J, Liu W, J. S. Allen JS, Song V, Wickline SA, Yu X. 2004. Dynamic alterations in myocardial fiber and laminar sheet structure of rat hearts in diastole and systole quantified by diffusion tensor MRI. In: *Proceedings of the 12th Annual Meeting of the International Society for Magnetic Resonance in Medicine (ISMRM 2004)*. p 649.
- Cromey D, Lantz C. 2015. Formaldehyde fixatives. SWEHSC Cellular Imaging Facility Core, Microscopy and Imaging Resources. <http://swehsc.pharmacy.arizona.edu/micro/formaldehyde>. Accessed 18 April 2015.
- Dyrby TB, Baaré WF, Alexander DC, Jelsing J, Garde E, Søgaard LV. 2011. An ex vivo imaging pipeline for producing high-quality and high-resolution diffusion-weighted imaging datasets. *Hum Brain Mapp* 32(4):544–563.
- Eggen MD, Swingen CM, Iaizzo PA. 2012. Ex vivo diffusion tensor MRI of human hearts: Relative effects of specimen decomposition. *Magn Reson Med* 67(6):1703–1709.
- Fox CH, Johnson FB, Whiting J, Roller PP. 1985. Formaldehyde fixation. *J Histochem Cytochem* 33(8):845–853.
- Giannakidis A, Rohmer D, Veress AI, Gullberg GT. 2012. Diffusion tensor magnetic resonance imaging-derived myocardial fiber disarray in hypertensive left ventricular hypertrophy: Visualization, quantification and the effect on mechanical function. In: Shenasa M, Hindricks G, Borggreffe M, Breithardt G, Josephson ME, editors. *Cardiac Mapping*. 4th ed.. Chichester: Wiley-Blackwell. p 574–588.
- Gilbert SH, Smaill BH, Walton RD, Trew ML, Bernus O. 2013. DT-MRI measurement of myolaminar structure: accuracy and sensitivity to time post-fixation, b-value and number of

directions. In: Proceedings of the 35th Annual International Conference of the IEEE Engineering in Medicine and Biology Society (EMBC 2013). p 699–702.

Guilfoyle DN, Helpert JA, Lim KO. 2003. Diffusion tensor imaging in fixed brain tissue at 7.0 T. *NMR Biomed* 16(2):77–81.

Hales PW, Burton RAB, Bollensdorff C, Mason F, Bishop M, Gavaghan D, Kohl P, Schneider JE. 2011. Progressive changes in T_1 , T_2 and left-ventricular histo-architecture in the fixed and embedded rat heart. *NMR Biomed* 24(7):836–843.

Helm PA, Younes L, Beg MF, Ennis DB, Leclercq C, Faris OP, McVeigh E, Kass D, Miller MI Winslow RL. 2006. Evidence of structural remodeling in the dyssynchronous failing heart. *Circ Res* 98(1):125–132.

Henwood AF. 2010. Osmolality and pH of neutral buffered formalin (NBF). *Biotech Histochem* 85(5):326–327.

Hernandez AM, Huber JS, Murphy ST, Janabi M, Zeng GL, Brennan KM, O'Neil JP, Seo Y, Gullberg GT. 2013. Longitudinal evaluation of left ventricular substrate metabolism, perfusion, and dysfunction in the spontaneously hypertensive rat model of hypertrophy using small-animal PET/CT imaging. *J Nucl Med* 54(11):1938–1945.

Hsu EW, Muzikant AL, Matulevicius SA, Penland RC, Henriquez CS. 1998. Magnetic resonance myocardial fiber-orientation mapping with direct histological correlation. *Am J Physiol Heart Circ Physiol* 274(5):H1627–H1634.

Hsu EW, Healy LJ, Einstein DR, Kuprat AP. 2009. Imaging-based assessment and modeling of the structures of the myocardium. In: Guccione JM, Kassab GS, Ratcliffe MB, editors. *Computational cardiovascular mechanics – modeling and applications in heart failure*. New York: Springer. p 23–39.

Jiang Y, Guccione JM, Ratcliffe MB, Hsu EW. 2007. Transmural heterogeneity of diffusion anisotropy in the sheep myocardium characterized by MR diffusion tensor imaging. *Am J Physiol Heart Circ Physiol* 293(4):H2377–2384.

Kim TH, Zollinger L, Shi XF, Rose J, Jeong EK. 2009. Diffusion tensor imaging of *ex vivo* cervical spinal cord specimens: The immediate and long-term effects of fixation on diffusivity. *Anat Rec* 292(2):234–241.

Klingberg T, Vaidya CJ, Gabrieli JDE, Moseley ME, Hedehus M. 1999. Myelination and organization of the frontal white matter in children: a diffusion tensor MRI study. *NeuroRep* 10(13):2817–2821.

Koay CG, Chang LC, Carew JD, Pierpaoli C, Basser PJ. 2006. A unifying theoretical and algorithmic framework for least squares methods of estimation in diffusion tensor imaging. *J Magn Reson* 182(1):115–125.

Li W, Lu M, Banerjee S, Zhong J, Ye A, Molter J, Yu X. 2009. *Ex vivo* diffusion tensor MRI reflects microscopic structural remodeling associated with aging and disease progression in normal and cardiomyopathic Syrian hamsters. *NMR Biomed* 22(8):819–825.

- Lombaert H, Peyrat JM, Croisille P, Rapacchi S, Fanton L, Cheriet F, Clarysse P, Magnin I, Delingette H, Ayache N. 2012. Human atlas of the cardiac fiber architecture: Study on a healthy population. *IEEE Trans Med Imaging* 31(7):1436–1447.
- Mazumder R, Choi S, Raterman B, Clymer BD, Kolipaka A, White RD. 2013a. Diffusion tensor imaging of formalin fixed infarcted porcine hearts. *J Cardiovasc Magn Reson* 15(Suppl 1):E103.
- Mazumder R, Choi S, Raterman B, Clymer BD, Kolipaka A, White RD. 2013b. Diffusion tensor imaging of formalin fixed infarcted porcine hearts: A comparison between 3T and 1.5T. *J Cardiovasc Magn Reson* 15(Suppl 1):W34.
- Mazumder R, Choi S, Clymer BD, White R, Kolipaka A. 2013c. Diffusion tensor imaging of fresh and formalin fixed porcine hearts: A comparison study of fiber tracts. In: *Proceedings of the 21st Annual Meeting of the International Society for Magnetic Resonance in Medicine (ISMRM 2013)*. p 2100.
- Papadakis NG, Xing D, Huang CL, Hall LD, Carpenter TA. 1999. A comparative study of acquisition schemes for diffusion tensor imaging using MRI. *J Magn Reson* 137(1):67–82.
- Schmierer K, Wheeler-Kingshott CA, Tozer DJ, Boulby PA, Parkes HG, Yousry TA, Scaravilli F, Barker GJ, Tofts PS, Miller DH. 2008. Quantitative magnetic resonance of postmortem multiple sclerosis brain before and after fixation. *Magn Reson Med* 59(2):268–277.
- Shepherd TM, Thelwall PE, Stanisz GJ, Blackband SJ. 2009. Aldehyde fixative solutions alter the water relaxation and diffusion properties of nervous tissue. *Magn Reson Med* 62(1):26–34.
- Srinivasan M, Sedmak D, Jewell S. 2002. Effect of fixatives and tissue processing on the content and integrity of nucleic acids. *Am J Pathol* 161(6):1961–1971.
- Streeter DD Jr, Spotnitz HM, Patel DP, Ross J Jr, Sonnenblick EH. 1969. Fiber orientation in the canine left ventricle during diastole and systole. *Circ Res* 24(3):339–347.
- Walker JC, Guccione JM, Jiang Y, Zhang P, Wallace AW, Hsu EW, Ratcliffe MB. 2005. Helical myofiber orientation after myocardial infarction and left ventricular surgical restoration in sheep. *J Thorac Cardiovasc Surg* 129(2):382–390.
- Wang J, Lin Y, Wai Y, Liu H, Lin C, Huang Y. 2008. Visualization of the coherence of the principal diffusion orientation: An eigenvector-based approach. *Magn Reson Med* 59(4):764–770.
- Watson BR, Hsu EW. 2012. Effects of formalin fixation on diffusion tensor imaging of myocardial tissues. In: *Proceedings of the 20th Annual Meeting of the International Society for Magnetic Resonance in Medicine (ISMRM 2012)*. p 1114.
- Webster JD, Miller MA, DuSold D, Ramos-Vara J. 2009. Effects of prolonged formalin fixation on diagnostic immunohistochemistry in domestic animals. *J Histochem Cytochem* 57(8):753–761.

Werner M, Chott A, Fabiano A, Battifora H. 2000. Effect of formalin tissue fixation and processing on immunohistochemistry. *Am J Surg Pathol* 24(7):1016–1019.

Wu EX, Wu Y, Nicholls JM, Wang J, Liao S, Zhu S, Lau CP, Tse HF. 2007. MR diffusion tensor imaging study of postinfarct myocardium structural remodeling in a porcine model. *Magn Reson Med* 58(4):687–695.

Wu Y, Chan CW, Nicholls JM, Liao S, Tse HF, Wu EX. 2009. MR study of the effect of infarct size and location on left ventricular functional and microstructural alterations in porcine models. *J Magn Reson Imaging* 29(2):305–312.

TABLES

Table 1 A summary of the quantitative results of the comparison study between rat hearts that were exposed to formalin for shorter (~2 weeks) and longer (~6-8 weeks) time intervals prior to imaging. All parameter values are group averages \pm standard deviations. λL = longitudinal diffusivity, λT = transversal diffusivity, MD = mean diffusivity, FA = fractional anisotropy, IVDC = inter-voxel diffusion coherence index, SNR = signal-to-noise ratio. All diffusivity values are expressed in mm^2/s .

FIGURE LEGENDS

Fig.1 Region of interest (ROI) averages of (a) transversal diffusivity (λT), (b) longitudinal diffusivity (λL), (c) mean diffusivity (MD), and (d) fractional anisotropy (FA) for all hearts ($N=8$) of this study. The cross symbol corresponds to rat hearts ($N=4$) that were exposed to formalin for a shorter time interval (namely, ~2 weeks) prior to imaging, while the diamond symbol represents samples ($N=4$) that remained

in formalin for a more prolonged time interval (namely, ~6-8 weeks) before imaging. ROI averages for each heart appear as symmetric error bars that are centered in the mean value and two standard deviations long. The unit of λT , λL , and MD is mm^2/s .

Fig.2 Visualization of helix angle (HA) maps from two representative rat hearts that were exposed to formalin for (a) a shorter time interval (namely, ~2 weeks) prior to imaging, and (b) a more prolonged time interval (namely, ~6-8 weeks) before imaging.

Fig.3 Group averages of the probability density functions (PDFs) of helix angles (HA) for the group of rat hearts ($N=5$) that were exposed to formalin for (a) a shorter time interval (namely, ~2 weeks) prior to imaging, and (b) a more prolonged time interval (namely, ~6-8 weeks) before imaging. The bin size was chosen to be 10 degrees. Group averages for each HA density bin are represented by symmetric error bars that are centered in the mean value and two standard deviations long. * indicates statistically significant differences ($p<0.05$).

Fig.4 Region of interest (ROI) averages of the inter-voxel diffusion coherence index (IVDC) for all hearts ($N=8$) of this study. The cross symbol corresponds to rat hearts ($N=4$) that were exposed to formalin for a shorter time interval (namely, ~2 weeks) prior to imaging, while the diamond symbol represents samples ($N=4$) that remained in formalin for a more prolonged time interval (namely, ~6-8 weeks) before imaging. ROI averages for each heart appear as symmetric error bars that are centered in the mean value and two standard deviations long.

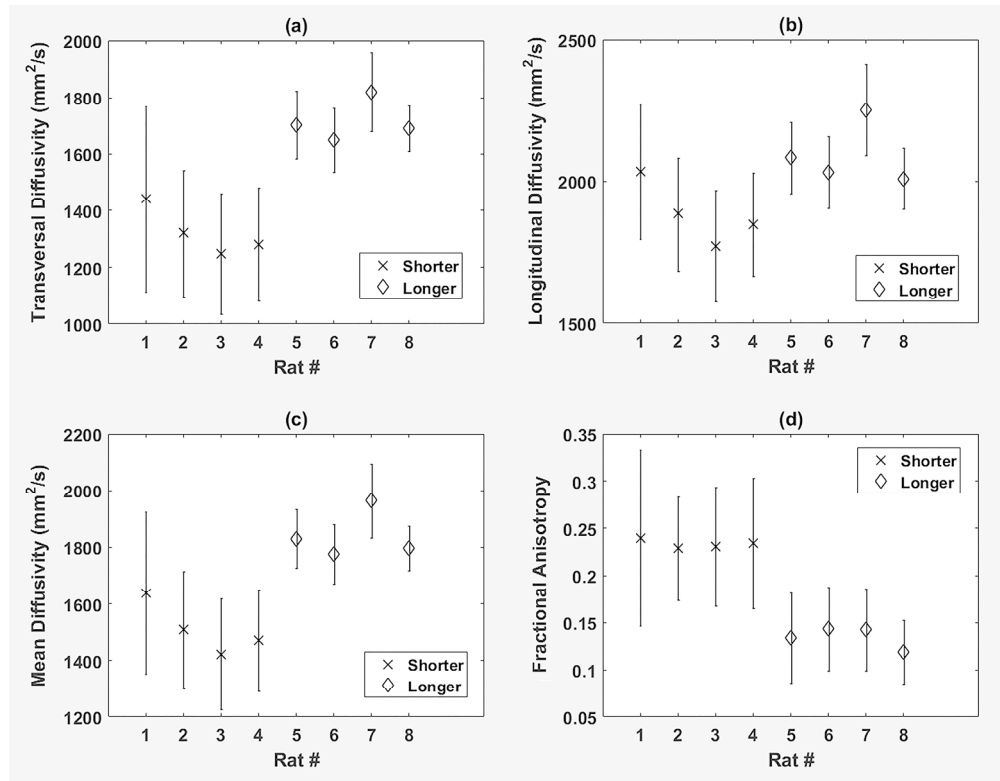


Figure 1 - Region of interest (ROI) averages of (a) transversal diffusivity (λ_T), (b) longitudinal diffusivity (λ_L), (c) mean diffusivity (MD), and (d) fractional anisotropy (FA) for all hearts (N=8) of this study. The cross symbol corresponds to rat hearts (N=4) that were exposed to formalin for a shorter time interval (namely, ~2 weeks) prior to imaging, while the diamond symbol represents samples (N=4) that remained in formalin for a more prolonged time interval (namely, ~6-8 weeks) before imaging. ROI averages for each heart appear as symmetric error bars that are centered in the mean value and two standard deviations long.

The unit of λ_T , λ_L , and MD is mm^2/s .

105x82mm (600 x 600 DPI)

Acce]

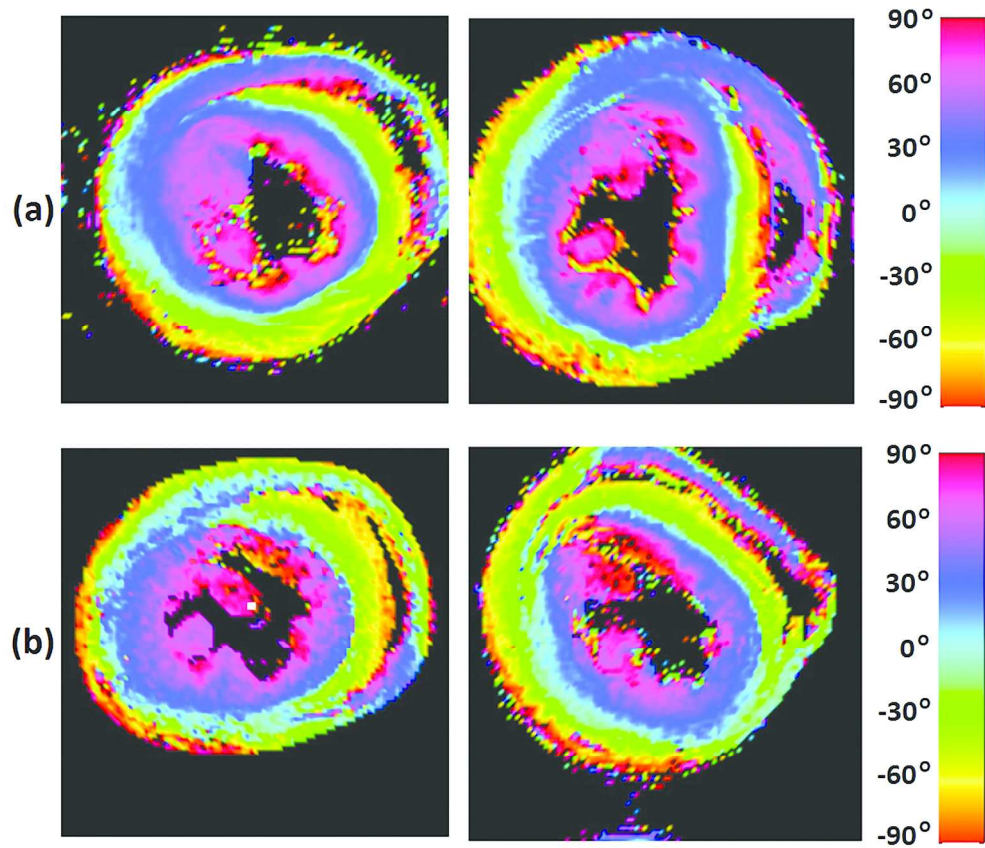


Figure 2 - Visualization of helix angle (HA) maps from two representative rat hearts that were exposed to formalin for (a) a shorter time interval (namely, ~2 weeks) prior to imaging, and (b) a more prolonged time interval (namely, ~6-8 weeks) before imaging.
232x199mm (300 x 300 DPI)

Accep

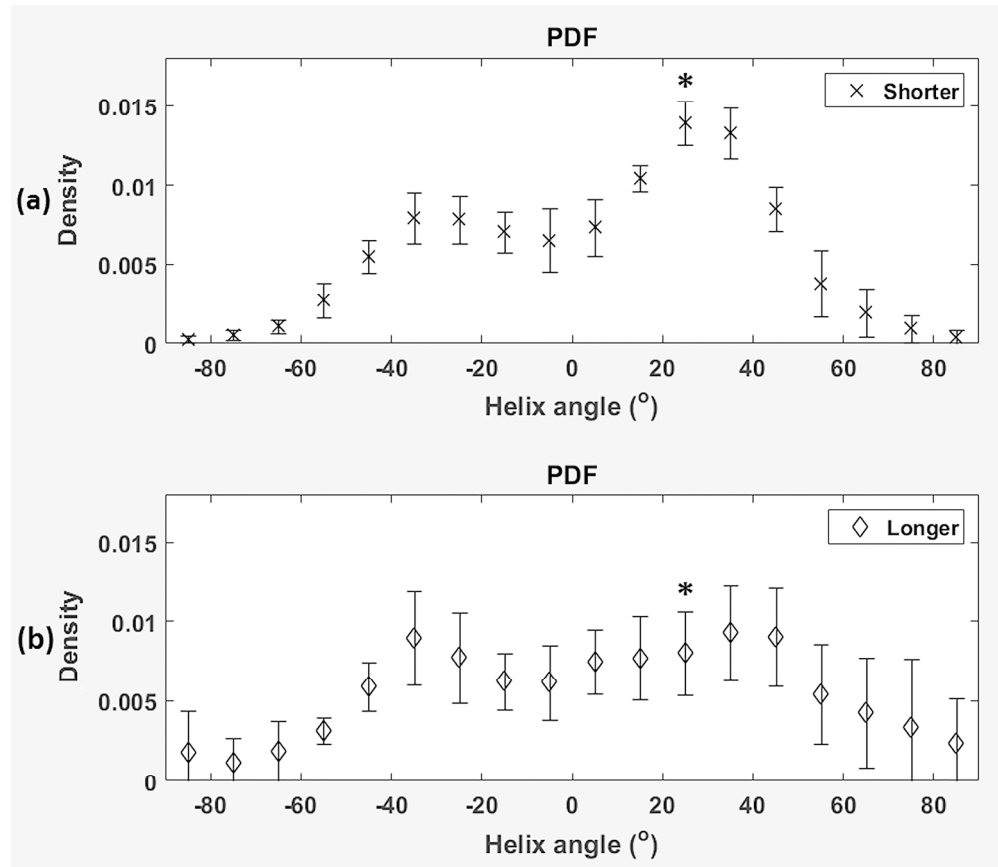


Figure 3 - Group averages of the probability density functions (PDFs) of helix angles (HA) for the group of rat hearts (N=5) that were exposed to formalin for (a) a shorter time interval (namely, ~2 weeks) prior to imaging, and (b) a more prolonged time interval (namely, ~6-8 weeks) before imaging. The bin size was chosen to be 10 degrees. Group averages for each HA density bin are represented by symmetric error bars that are centered in the mean value and two standard deviations long. * indicates statistically significant differences ($p < 0.05$).

116x100mm (600 x 600 DPI)

Acce

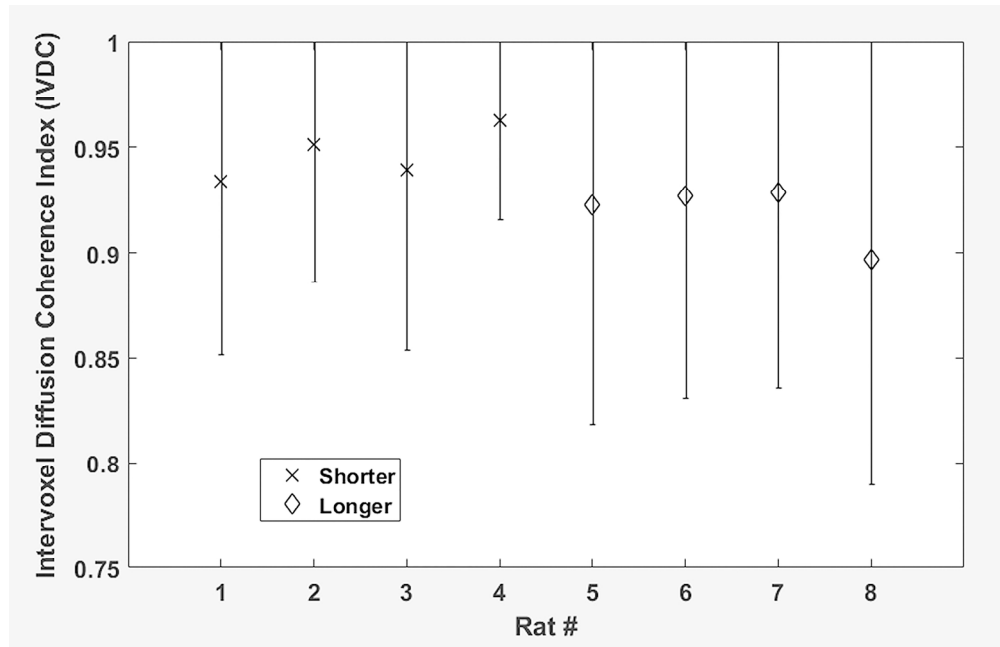


Figure 4 - Region of interest (ROI) averages of the inter-voxel diffusion coherence index (IVDC) for all hearts (N=8) of this study. The cross symbol corresponds to rat hearts (N=4) that were exposed to formalin for a shorter time interval (namely, ~2 weeks) prior to imaging, while the diamond symbol represents samples (N=4) that remained in formalin for a more prolonged time interval (namely, ~6-8 weeks) before imaging. ROI averages for each heart appear as symmetric error bars that are centered in the mean value and two standard deviations long.

93x59mm (600 x 600 DPI)

Accept

Table 1

	Shorter	Longer	<i>p</i> -value
λL	1885 \pm 110	2094 \pm 110	0.1143
λT	1323 \pm 84	1716 \pm 73	<0.05
MD	1510 \pm 93	1842 \pm 84	<0.05
FA	0.2334 \pm 0.0049	0.1348 \pm 0.0113	<0.05
IVDC	0.9467 \pm 0.0128	0.9188 \pm 0.0150	<0.05
SNR	119 \pm 13	143 \pm 10	0.0571